Unveiling the Moon : Lunar elemental cartography using Chandrayaan 2

Team 57

[a] *Inter IIT Tech Meet,*

Abstract

This report details the advancements made in the project focused on achieving **high-Resolution Elemental Mapping of the Lunar Surface**. Using data from the CLASS instrument on Chandrayaan-2, we have developed a comprehensive catalog of detected X-ray fluorescence (XRF) lines along with their corresponding elemental identifications, governed by the relevant source codes used in the analysis. Consequently, we have successfully mapped the coverage of these XRF lines onto a lunar base map, providing a spatial overview of elemental distribution across the lunar surface and different types of compositional groups has been identified from the calculated ratios. The latter part of the work encompasses generation of an interactive map and a heat map of various elements projected on the lunar surface as the final end product.

Keywords: XRF, Lunar surface mapping, Elemental abundance

1. Introduction

X-ray fluorescence (XRF) spectroscopy is a powerful analytical technique widely used determining the elemental composition of surfaces in a non-destructive manner. for the space based approaches, Sun acts as the main source of X-rays and characteristic X-ray emissions generated when a material is excited by an external X-ray source. XRF allows for the precise identification and quantification of elements within a area. When the surface of an airless body is exposed to solar X-rays or cosmic rays, the atoms in the surface materials absorb energy and re-emit it as fluorescent X-rays characteristic of each element. Instruments like the Chandrayaan-2 Large Area Soft X-ray Spectrometer (CLASS) use this principle to detect elemental XRF lines and map surface compositions from orbit.

To understand the lunar formation and its geological evolution, the Lunar surface composition mapping has been a measure target since the ignition of lunar exploration. Nearly 20% of lunar surface has been mapped by Apollo 15 and 16 XRF experiments by Mg/Si and Al/Si ratios. Chandrayaan-1 X-ray spectrometer (C1XS) [3] has already determined elemental abundances of about 5% of the moon.

Launched on July 22nd, 2019 by GSLV MkIII-M1 rocket from Satish Dhawan Space Centre Sriharikota, the Chandrayaan-2 mission marked an important milestone for India's lunar exploration. The Chandrayaan-2 Large Area Soft X-ray Spectrometer (CLASS) analyzes the moon's surface composition b y measuring the XRF spectra. Elements like Magnesium, Silicon, Aluminum, Calcium, Titanium, Iron and Sodium, by detecting characteristics spectral emissions.

2. Methodology

2.1. Catalogue of XRF Line detection

We are using data from the CLASS solar XRF data archive at [4]. We chose particular spectral files corresponding to a particular solar flare event according to the XSM data archive. In this spectral data, when we are encountering bad statistics, corresponding spectra are added up in a time sequential manner until we get good statistics. In our final albedo map we plan to use the entirety of the XSM data and identify peak points for corresponding suitable lunar XRF spectra detections.

For each particular FITS file with XRF spectra, we identify the energy bounds of the metals detected by referring to the NIST database [7] for energy values of various metals in their different transitions. We do a preliminary estimate of the number of lines detected for each of these elements (if present at all).

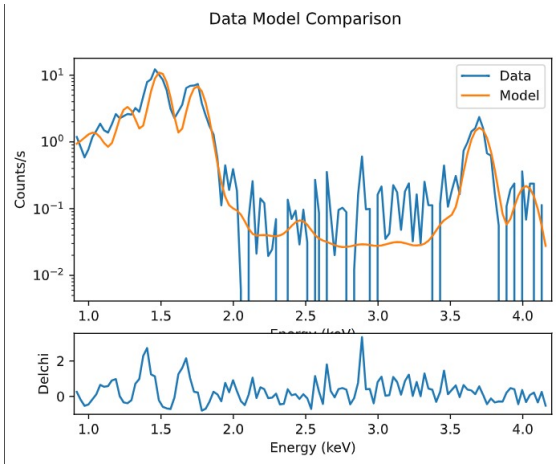

Figure 1: X2Abundance Model [7] fit of XRF using Xspec

We also calculate the scattered solar spectrum for our time interval of data used from XSM spectral data provided The provided re-distribution matrix file (RMF) and ancillary response file (ARF) are used in model fitting the corresponding spectra. The first estimate from the signal data for estimating

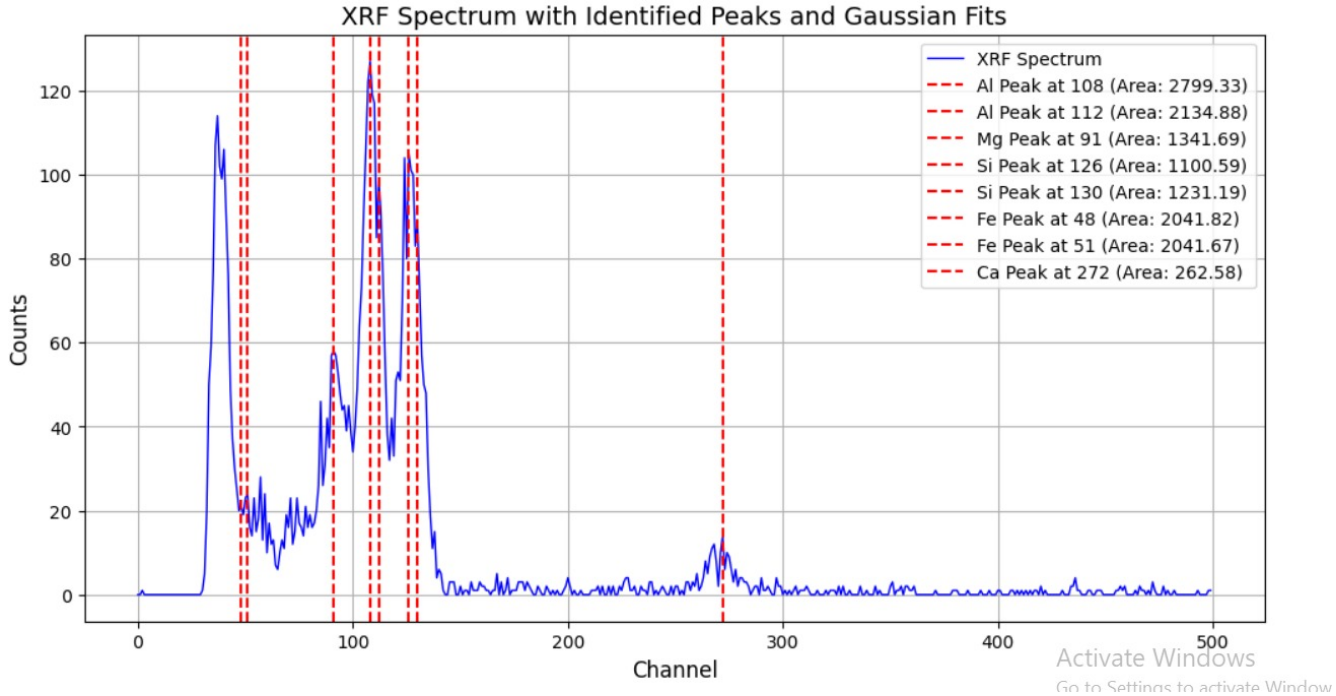

Figure 2: Multiple Gaussian fit to get the rough estimate of number of lines and area under each elemental curve

number of lines is conducted via a multiple Gaussian fit analysis and the area is computed to obtain the total flux of each element. (Shown in figure 1) We plan to extend this approach by using Bayesian Estimation Method in XSpec [6] using the X2Abundance Model for all files. (Figure 2). We identify the fluxes and take ratios of Mg/Si, Al/Si, Ca/Si, Fe/Si, Ti/Si, Fe/Mn and Ca/Al in our catalog.

2.2. Lunar Mapping the coverage of XRF lines

It is observed that the CLASS data covers almost 95% of the lunar surface but we are concerned with the particular tracks where there are solar flare events for we get good XRF line detections from these coordinates exclusively.

2.2.1. Data Collection and Initial Filtering

Downloading Files : We have downloaded all the fits file from the "Pradan" website [**<empty citation>**] and all the fits file contains the useful coordintes of the four corners creating a box.

Parsing XML Files :

- `xml.etree.ElementTree` (referred to as xml.etree) from Python was isued to parse the XML files which contains all the meta-datas associated with each fits file.
- After the parsing of data is done, we were able to extract the four cordinates of the corner points for the particular region. Additionally, we have gone through the date and time information from the filenames as documented in the CH-2 user manual [9].
- Now the parsed information, including all its attributes was saved in a CSV file, which worked as a heart of the whole work, that enables a quick access to geographical and temporal information for each fits file while matching datas with Solar flare datas.

2.2.2. Filtering Based on Solar Flares:

- Using Solar Flare Database (XSM) we cross checked and took it as a refrenece to our fits data, which records flare events and their energy spectra over time.
- Spectrum Selection was a measure part of these works so for analysis, we looked into those events who had high energy flare flux to get a distinguishable XRF spectra which helped us in identification of elements focused on high-energy flare events, as these produce clearer and more distinguishable XRF spectra, enabling easier identification of lunar elements.

2.2.3. Loading the Lunar Base Map:

- We have used rasterio to load the lunar base map (`lunar_base_image.tif`) using `rasterio.open()`. `lunar_image = src.read(1)` This reads the base map file in 2D array.
  `lunar_extent = (src.bounds.left, src.bounds.right, src.bounds.bottom, src.bounds.top)` helps to capture spatial extent.
  So the file is used as the base map over which we overlayed the XRF coverage.

2.2.4. Work Flow :

- We have used solar flare datas (SD_GOES and SD_CH2 in the submission) as input files to get a intermediate CSV file to be processed further.
- This file along with a file (all_latlong_data in the submission) given to a python code to get final CSV file which is used for final mapping.
- we got the out plotten map as both PNG and TIFF files (Provided in the submission)

The final image obtained after lunar base mapping is show in figure 3.

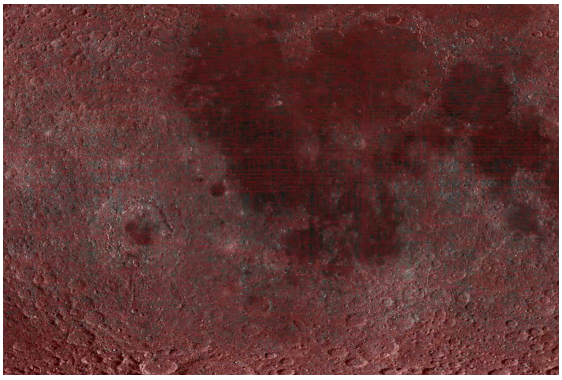

Figure 3: Lunar base map coverage of XRF lines

2.3. Compositional Groups Based on Ratios

Research until now suggests that lunar surface is mostly abundant with Silicon, Magnesium, Calcium, Aluminum and Titanium, but oxygen is most abundant in the minerals in the rocks. Minor elements like Sodium, Manganese, Phosphorous, Potassium were also found in very less number. According to previous studies the following minerals are majorly found on lunar crust :

Composition Group	**Description**
Pyroxene	Calcium, Iron, Magnesium Silicate compositional group.
Clinopyroxene	Pyroxene subgroup containing Calcium with a wide range of composition.
Orthopyroxene	Typically higher in Magnesium and Iron, with little Calcium.
Olivine	Magnesium-Iron Silicate compositional group.
Ilmenite	Iron-Titanium Oxide compositional group.
Feldspar	Aluminum-Silicate compositional group.
Plagioclase	Calcium-Sodium-Aluminum Silicate form of feldspar.
Anorthite	Calcium-rich plagioclase subgroup.

2.3.1. Work Flow

section We have derived the percentage of different elements from the XRF datas. We have used an approximate composition CSV table to match the percentage derived in the XRF analysis.

- We have defined a measuring parameter "Score" which actually defines the standard deviation in ratios.
- The score is defined as
  $\text{score} = \sqrt{\sum_i (\text{data\_ratio}_i - \text{group\_ratio}_i)^2}$
- Lesser the standard deviation we call the particular area defined by the particular fits file will have a possibility of holding such compositional group.

3. Interactive mapping

Due to the presence of rich data for a particular small area of 12.5 km × 12.5 km the visualization can be conducted precisely on an interactive map. Here each points describe the relative ratio of each element with Silicon and the weight % of each element is displayed. Our code generates an interactive map of the lunar surface using the Plotly library. We have used the derived weight percentages and ratios calculated earlier from the flux of the XRF spectral data and placed it over a lunar albedo map. The figure given below is a snippet of the same.

Figure 4: Interactive Map Example

4. Sub-pixel resolution

The nature of the XRF line coverage correspond to numerous overlap of data for given parts of grids. The properties of these overlapped areas will give sub-pixel data and accurate visualization of divergences within the grid. So while showing the interactive map we are creating two different points for the region. The property for the two different points are given by the averages. Instead of a whole $12.5km \times 12.5km$ box property we will have more number of points due to the overlaps inside this box resulting into smaller boxes inside this core $12.5km \times 12.5km$.

5. Heat map

Once we have the relative weight percentages of our elements of interest, we can have a contour or a heat map of the lunar surface corresponding to each of these elements. We have observed good structural correlations in different elements of the heat maps which agree with geological findings. The heat maps of Al, Mg, Si, Fe and Ca are attached where correlated and anti-correlated structures can be evidently observed.

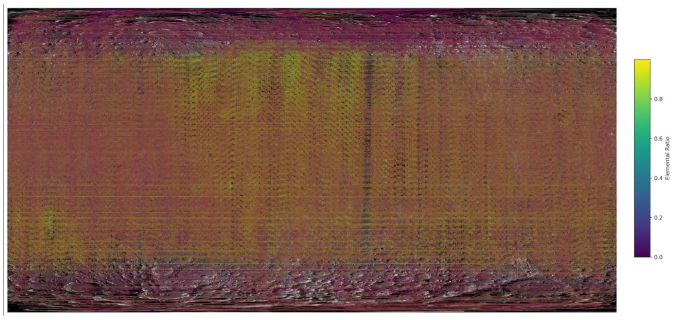

Figure 5: Mg Coverage map

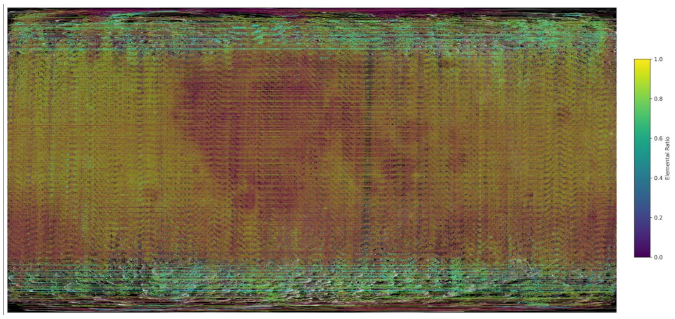

Figure 6: Al Coverage map

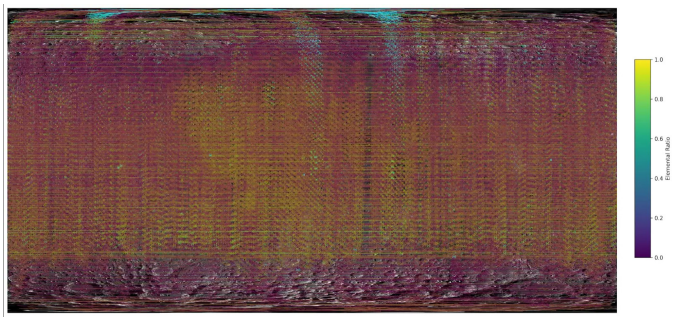

Figure 7: Fe Coverage Map

6. Results and Summary

- The XRF CLASS datas were analyzed and a catalog has been created containing the element ratios and the normalized ratio of the element has been derived.

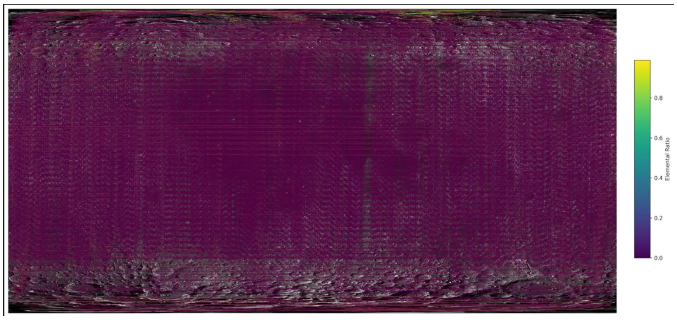

Figure 8: Ca Coverage map

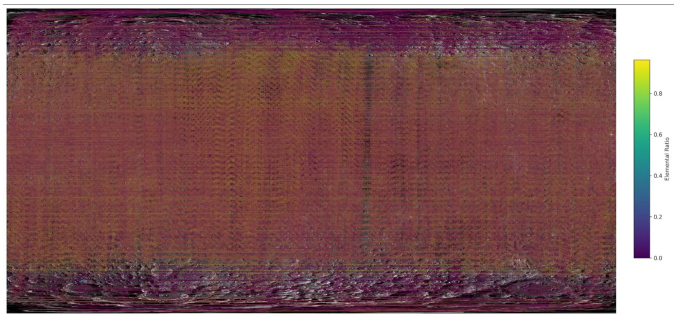

Figure 9: Si Coverage Map

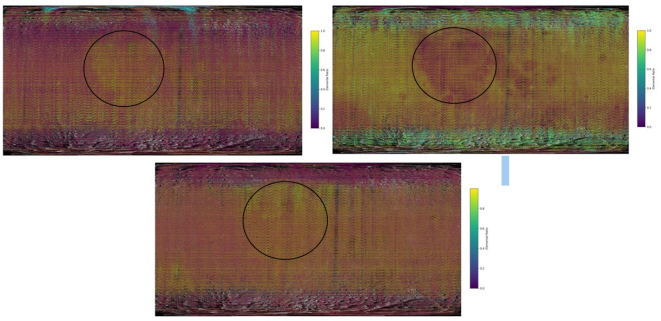

Figure 10: Co-relation between Fe-Al-Mg

- Using both XSM and GOES datas for the significant solar flares we got useful XRF datas from which after extracting the co-ordinates we plotted on a lunar basemap. from The elemental ratios we have assigned each fits file with some compositional groups corresponding to the best fit deviation.

7. Future Prospects

GAN based methods have been increasingly gaining traction in the field of image analysis for super-resolution and have shown considerable improvements in image resolution [1]. In [2] the MFSR (Multi-Frame Super Resolution Method) was used to train a deep learning architecture on the LRO (Lunar Reconnaissance Orbiter) mission data for super resolution. There have also been advances in the application of deep learning networks for cosmological simulation models to achieve better resolution [5].

In the case of the CLASS lunar XRF data it will be novel and interesting to integrate a deep learning-assisted super-resolution generative adversarial network (Deep SRGAN) which could potentially help in resolving data much beyond the pixel resolution limit of the device.

Statistical learning methods used in experimental particle physics [8] are also very relevant in signal detection techniques on XRF elemental spectra. We can have coherent signal/background discrimination tasks using supervised learning to direct data-driven approaches, as we know the theoretical transition values of the elements in which we are interested.

References

[1] Chunwei Tian and Xuanyu Zhang and Jerry Chun-Wei Lin and Wangmeng Zuo and Yanning Zhang and Chia-Wen Lin. *Generative Adversarial Networks for Image Super-Resolution: A Survey*. 2022. URL: https://arxiv.org/abs/2204.13620.

[2] Delgado-Centeno, J. I. and Sanchez-Cuevas, P. J. and Martinez, C. and Olivares-Mendez, M.A. *Enhancing Lunar Reconnaissance Orbiter Images via Multi-Frame Super Resolution for Future Robotic Space Missions*. URL: https://ieeexplore.ieee.org/document/9488313.

[3] Grande M., Maddison B.J., Howe C.J., Kellett B.J., Sreekumar P., Huovelin J., Crawford I.A., Duston C.L., Smith D., Anand M., Bhandari N., Cook A., Fernandes V., Foing B., Gasnaut O., Goswami J.N., Holland A., Joy K.H., Kochney D., Lawrence D., Maurice S., Okada T., Narendranath S., Pieters C., Rothery D., Russell S.S., Shrivastava A., Swinyard B., Wilding M., Wieczorek M. *The C1XS X-ray spectrometer on Chandrayaan-1*. 2016.

[4] ISRO. *CLASS DATA*. 2019-2024. URL: https://pradan.issdc.gov.in/.

[5] Li, Yin and Ni, Yueying and Croft, Rupert A. C. and Di Matteo, Tiziana and Bird, Simeon and Feng, Yu. *AI-assisted superresolution cosmological simulations*. 2021. URL: http://dx.doi.org/10.1073/pnas.2022038118.

[6] NASA. *Xspec Home Page*. URL: https://heasarc.gsfc.nasa.gov/xanadu/xspec/.

[7] NIST. *X-Ray Transition Energy Database*. URL: https://physics.nist.gov/PhysRefData/XrayTrans/Html/search.html.

[8] Schwartz, Matthew D. *Modern Machine Learning and Particle Physics*. 2021. URL: https://doi.org/10.48550/arXiv.2103.12226.

[9] SPACE ASTRONOMY GROUP, UR RAO SATELLITE CENTRE, ISRO. *CLASS USER MANUAL*. 2021. URL: https://pradan.issdc.gov.in/ch2/protected/downloadFile/class/ch2_class_pds_release_38_20240927.zip.